PERGAMON

International Journal of Solids and Structures 36 (1999) 1427–1447

INTERNATIONAL JOURNAL OF SOLIDS and STRUCTURES

A finite element investigation of the effect of crack tip constraint on hole growth under mode I and mixed mode loading

Y. Arun Roy, R. Narasimhan*

Department of Mechanical Engineering, Indian Institute of Science, Bangalore 560 012, India

Received 2 July 1997; in revised form 16 January 1998

Abstract

In this work, the effect of constraint on hole growth near a notch tip in a ductile material under mode I and mixed mode loading (involving modes I and II) is investigated. To this end, a 2-D plane strain, modified boundary layer formulation is employed in which the mixed mode elastic K–T field is prescribed as remote boundary conditions. A finite element procedure that accounts for finite deformations and rotations is used along with an appropriate version of J_2 flow theory of plasticity with small elastic strains. Several analyses are carried out corresponding to different values of T-stress and remote elastic mode-mixity. The interaction between the notch and hole is studied by examining the distribution of hydrostatic stress and equivalent plastic strain in the ligament between the notch tip and the hole, as well as the growth of the hole. The implications of the above results on ductile fracture initiation due to micro-void coalescence are discussed.

1. Introduction

Ductile fracture in metallic alloys begins with the nucleation of cavities from brittle cracking or decohesion of inclusions. These cavities grow in size due to plastic deformation in the surrounding material. The growth of the cavities is strongly influenced by high triaxial tension. Several studies (see, for example, Aravas and McMeeking, 1985a, b; Ghosal and Narasimhan, 1996) have been undertaken to model the void growth process with the view of understanding the micro-mechanics of ductile fracture. Aravas and McMeeking (1985a, b) have used a finite element model of a notch with a circular hole placed ahead of it, in order to investigate the growth of the hole caused by its interaction with the notch tip under mode I loading. Using a similar approach, Ghosal and Narasimhan (1996) have examined several issues concerned with the mixed mode fracture of

* Corresponding author. Fax: 91803341683; e-mail: narasi@mecheng.iisc.ernet.in

0020–7683/99/$ - see front matter
PII: S0020–7683(98)00046–8

ductile materials. In their work, the background material response was represented by the Gurson constitutive equation (Gurson, 1977), and the failure of the ligament connecting the notch tip and the hole by either micro-void coalescence or shear localization was modelled. Thus, the competition between the above two failure mechanisms in promoting mixed mode ductile fracture was simulated and the variation of the critical value of the J-integral at fracture initiation with mode mixity was predicted. The effect of initiation of a discrete void by inclusion debonding on mixed mode ductile fracture was examined by Ghosal and Narasimhan (1997). In all the above studies, attention was restricted to plane strain, small scale yielding conditions.

Recent research work (see, for example, Betegon and Hancock, 1991; O'Dowd and Shih, 1991) on plane strain, elastic–plastic fracture mechanics has brought out the limitations of a single parameter characterization (using J) of the crack tip fields in several mode I geometries (like, the centre cracked panel, single edge notch (tension), etc.). It was found that in these geometries, the J-controlled HRR fields do not dominate over length scales comparable to the material microstructure due to loss of crack tip constraint (or triaxiality). Betegon and Hancock (1991) have suggested that the near-tip stress and strain variations be characterized by J (or K) and T, where T is the second term in William's (1957) asymptotic expansion. They found J-dominance is maintained for zero or positive T-stress, while negative T-stress causes a loss of J-dominance which also reflects in loss of constraint or triaxiality near the crack tip. O'Dowd and Shih (1991, 1992) have proposed an alternate approach to quantify crack tip constraint. They suggested that J and a hydrostatic stress parameter, Q, be employed to describe the crack tip fields which was found to be adequate for a range of geometries and loading. Under conditions of small to intermediate scale yielding, the above two approaches are equivalent because a one to one relationship exists (O'Dowd and Shih, 1991, 1992) between T and Q. Further, Xia and Shih (1995a, b) and Tvergaard and Hutchinson (1994) have observed that crack tip constraint (or crack geometry) can significantly affect the crack growth resistance curves.

In a recent work, O'Dowd (1995) employed a fracture criterion based on the attainment of a critical crack tip opening displacement and predicted that the value of the fracture toughness for ductile tearing is lower if the T-stress (or Q-stress) is negative. However, the model employed by O'Dowd (1995) is too simplistic, because the process of ductile failure is triggered by plastic flow localization in the ligaments connecting the notch tip with nearby voids (Van Stone et al., 1985, Garrison and Moody, 1987). The growth of such voids is expected to be influenced by both plastic strain and triaxial stress prevailing near the notch tip. Hence, it is imperative that predictions of ductile fracture initiation be based on a study of the interaction between a notch tip and adjacent voids (as in Rice and Johnson, 1970; Aravas and McMeeking, 1985a, b; Ghosal and Narasimhan, 1996).

In a very recent work, Arun Roy and Narasimhan (1997) have used a modified boundary layer formulation to investigate the effect of T-stress on J-dominance in mixed mode elastic–plastic fracture mechanics. They found that, for a given remote elastic mode mixity $\Psi = \tan^{-1}(K_I/K_{II})$, the imposition of a non-zero T-stress changes the near-tip plastic mode mixity (which essentially represents the ratio of the normal to shear traction on the plane ahead of the tip) from its value corresponding to pure small scale yielding ($T = 0$; see Shih, 1974). This alters the stress triaxiality near the crack tip. However, it was found that except for loadings close to mode I, there is no loss of J-dominance if the stress fields are compared with the asymptotic mixed mode solution of Shih (1974) corresponding to the actual plastic mode mixity prevailing near the crack tip. Nevertheless,

the modification in near-tip plastic mode mixity due to imposition of the remote T-stress can affect the ductile fracture process near the crack tip. Very little research has been devoted so far to investigate the effect of crack tip constraint on ductile fracture initiation under mixed mode loading.

The present work is aimed at studying the effect of crack tip constraint on hole growth near a notch tip under mode I and mixed mode loading conditions. To this end, large deformation elastic–plastic finite element analyses are performed using a 2-D plane strain, modified boundary layer formulation. Here, the mixed mode elastic K–T field is prescribed as remote boundary conditions. The analyses are conducted for different values of T-stress and remote elastic mixities. The interaction between the notch and a nearby hole is studied by examining the distribution of hydrostatic stress and equivalent plastic strain in the ligament connecting them, as well as, the growth of the hole. The implications of these results on the effect of T-stress on the ductile fracture toughness are discussed.

2. Numerical procedure

In this work, an Updated Lagrangian finite element procedure (McMeeking and Rice, 1975) is employed. In this procedure, the reference configuration is taken to coincide instantaneously with the current configuration, so that the Kirchhoff stress τ_{ij} and Cauchy stress σ_{ij} are the same, whereas their rates are different. The finite element equations for rate equilibrium are derived from the following virtual work principle (see McMeeking and Rice, 1975):

$$\Delta t\int_{V_t}[\tau_{ij}^{*}-(\tau_{ik}D_{kj}+D_{ik}\tau_{kj})]\delta D_{ij}\,\mathrm{d}V+\Delta t\int_{V_t}\tau_{ij}v_{k,j}\delta v_{k,i}\,\mathrm{d}V=\Delta t\int_{V_t}\dot{b}_j\delta v_j\,\mathrm{d}V$$
$$+\Delta t\int_{S_T}\dot{T}_j\delta v_j\,\mathrm{d}A+\left[\int_{V_t}b_j\delta v_j\,\mathrm{d}V+\int_{S_T}T_j\delta v_j\,\mathrm{d}A-\int_{V_t}\sigma_{ij}\delta D_{ij}\,\mathrm{d}V\right]. \quad (1)$$

In this equation, all integrations are performed over the volume V_t and boundary segment S_T in the equilibrium configuration at time t, and $v_{k,i}=\partial v_k/\partial x_i$ is the spatial gradient of particle velocity vector. Also δv_i is a virtual velocity field which is imposed on the current equilibrium configuration and $\delta D_{ij}=1/2(\delta v_{i,j}+\delta v_{j,i})$ denotes the associated virtual rate of deformation tensor. Further, τ_{ij}^{*} is the Jauman rate of Kirchhoff stress and $\dot{b}_j$, $\dot{T}_j$ represent nominal body force and surface traction rates based on the current volume and surface area. It should be noted that eqn (1) applies strictly in a rate sense and, thus, the time step size Δt is viewed here to be very small. The term in square bracket on the right hand side of eqn (1) is an equilibrium correction term that vanishes when the known state at time t is an exact equilibrium state.

In this work, rate independent elastic–plastic constitutive equations which satisfy incremental objectivity are considered and are assumed to have the following structure:

$$\tau_{ij}^{*}=M_{ijkl}D_{kl}, \quad (2)$$

where, M_{ijkl} is the elastic–plastic constitutive tensor. The constitutive tensor M_{ijkl} for material obeying a finite strain version of the J_2 flow theory of plasticity (with small elastic strains) along with isotropic strain hardening is given by McMeeking and Rice (1975). The true stress vs true strain response under uniaxial tension is assumed to be of power law type in the form:

$$\frac{\varepsilon}{\varepsilon_0} = \left(\frac{\sigma}{\sigma_0}\right), \quad \sigma \leqslant \sigma_0$$

$$= \left(\frac{\sigma}{\sigma_0}\right)^n, \quad \sigma > \sigma_0, \tag{3}$$

where, σ_0 is the initial yield stress and $\varepsilon_0 = \sigma_0/E$ is the initial yield strain. The value of ε_0 and strain hardening exponent n are taken here as 0.002 and 10, respectively.

The B-bar method (Hughes, 1980) is employed here within the context of four-noded plane strain quadrilateral elements, since the deformation becomes nearly incompressible, which cannot be adequately modelled by the conventional displacement formulation. Further, the Hughes and Winget (1980) algorithm is used in this work to treat finite rotation effects, so that incremental objectivity is maintained during constitutive update.

3. Computational model

A large circular domain containing a notch along one of its radii, which is entirely represented by 2-D plane strain, four-noded, isoparametric quadrilateral elements is considered. The radius of the outermost boundary of this circular domain, r_0, is about $10^5 b_0$, where b_0 is the initial diameter of the notch. In the undeformed configuration, the centre of curvature of the notch coincides with the centre of the circular domain. A set of Cartesian coordinates (X_1, X_2) and polar coordinates (r, θ) are established with the origin at the centre of curvature O of the notch in the undeformed configuration as indicated in Fig. 1.

A typical mesh used to model the region near the notch tip is shown in Fig. 1. In this mesh, a circular (cylindrical) hole of diameter $a_0 = b_0$ has been placed at a distance $L = 5b_0$ directly ahead of the notch tip (i.e., at $\theta = 0^\circ$). The size of the smallest elements near the notch tip and the hole in this mesh is about $0.02L$. Further, it must be noted that elements having an almost regular shape have been employed in the ligament between the notch tip and the hole. A convergence study was performed by refining the elements near the notch tip and the hole and varying the number of elements in the ligament connecting them. From this study, it was found that converged results are obtained from the mesh depicted in Fig. 1. In addition to the case shown in Fig. 1, analyses have also been conducted using a finite element model with a hole placed at an angle of $\theta = -30^\circ$ and at the same distance L from the notch tip.

The displacement components based on the first two terms of the mixed mode elastic crack tip field which are given by,

$$u_1 = \left(\frac{r_0}{2\pi}\right)^{1/2} \frac{(1+\nu)}{E} \left\{ K_{\mathrm{I}} \cos\frac{\theta}{2}\left(\kappa - 1 + 2\sin^2\frac{\theta}{2}\right) + K_{\mathrm{II}} \sin\frac{\theta}{2}\left(\kappa + 1 + 2\cos^2\frac{\theta}{2}\right)\right\} + \frac{(1-\nu^2)}{E} T r_0 \cos\theta, \tag{4}$$

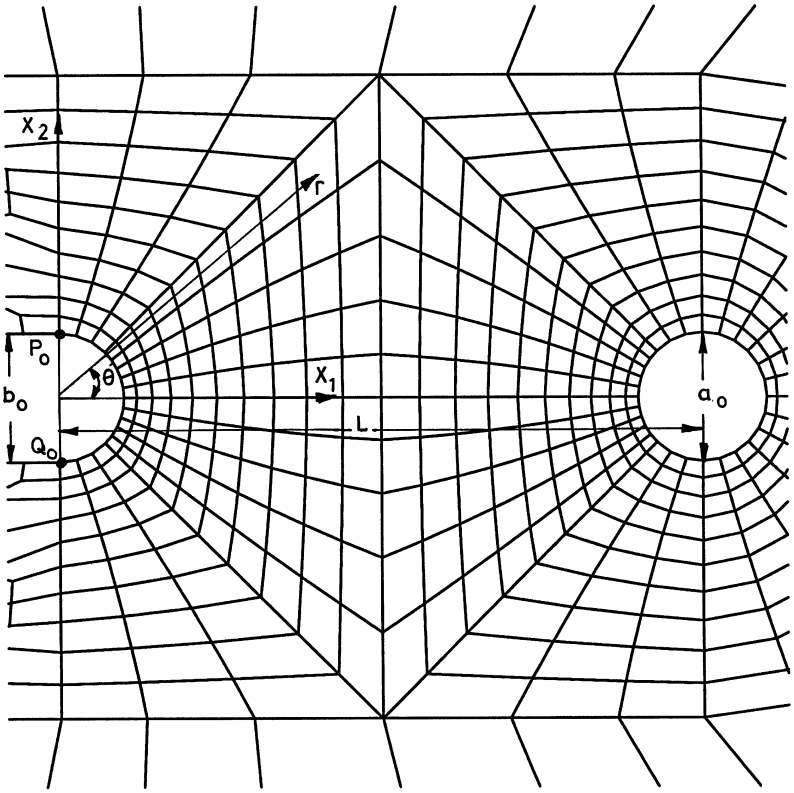

Fig. 1. Finite element mesh used near the notch tip and the hole in the computations.

$$u_2 = \left(\frac{r_0}{2\pi}\right)^{1/2} \frac{(1+\nu)}{E} \left\{ K_{\mathrm{I}} \sin\frac{\theta}{2}\left(\kappa + 1 - 2\cos^2\frac{\theta}{2}\right) - K_{\mathrm{II}} \cos\frac{\theta}{2}\left(\kappa - 1 - 2\sin^2\frac{\theta}{2}\right)\right\} - \frac{\nu(1+\nu)}{E} T r_0 \sin\theta, \quad (5)$$

are prescribed on the outer boundary of the domain. In the above equation, K_{I} and K_{II} are the mode I and II stress intensity factors, respectively. Further, E and ν (which is taken as 0.3) are the Young's modulus and the Poisson's ratio, and $\kappa = 3-4\nu$ for plane strain. The loading is applied in steps by gradually increasing the effective stress intensity factor $|K| = \sqrt{(K_{\mathrm{I}}^2 + K_{\mathrm{II}}^2)}$, while keeping T/σ_0, as well as the remote elastic mode mixity, $\Psi = \tan^{-1}(K_{\mathrm{I}}/K_{\mathrm{II}})$ fixed throughout a particular analysis. As in the work of Tvergaard and Hutchinson (1994), the value of T/σ_0 is first increased to the desired level and then held fixed in the remaining part of the analysis during which the effective stress intensity factor $|K|$ is increased. From numerical experimentation, it was found that this technique produces results which are similar to a method in which a constant biaxiality parameter $T/|K|$ is employed during the loading.

The accuracy of computations is continuously monitored by checking the magnitude of the out-

of-balance forces which signify the deviation from equilibrium [see terms within square bracket in the right hand side of eqn (1)], and very small increments in $|K|$ are used whenever this deviation is found to be large. Analyses are conducted with different ratios $T/\sigma_0 = -0.75$, 0, and $+0.75$ corresponding to several values of Ψ. The maximum extent of the plastic zone surrounding the notch tip is at all times contained well within the radius of the circular domain (less than 1/50), so that small scale yielding conditions are preserved. This was confirmed by continuously checking the value of the J-integral computed on contours remote from the crack tip with the far-field applied value which is given by $(1-\nu^2)|K|^2/E$. Static condensation is employed to reduce the degrees of freedom corresponding to the nodes lying in the far-field elastic region.

4. Results and discussion

4.1. *Deformed shapes of notch and hole*

In Figs 2(a) and (b), the deformed shapes of the notch and hole at different stages of loading for the mixed mode case, $\Psi = 45^\circ$ are shown corresponding to $T/\sigma_0 = +0.75$ and -0.75, respectively. In these and the following figures, the loading is indicated by the normalized parameter $J/(\sigma_0 L)$, where J is the J-integral which is obtained from the remote imposed stress intensity factors K_I and K_{II} as $J = (1-\nu^2)(K_I^2 + K_{II}^2)/E$. It can be seen from Fig. 2(a) that, for the case of positive T-stress, there is a mild sharpening of the top surface of the notch, while the remaining part blunts significantly and advances towards the hole. By contrast, it can be observed from Fig. 2(b) that, there is considerable sharpening of the top surface of the notch when the T-stress is negative. On examining the hole shape in Fig. 2(a) (for the case $T/\sigma_0 = +0.75$), it can be noticed that, it remains rounded and is gradually pulled away from the notch as $J/(\sigma_0 L)$ increases. For the case of negative T-stress (Fig. 2(b)), the hole elongates along an inclined axis and is pulled towards the blunted part of the notch.

4.2. *Distribution of hydrostatic stress and plastic strain in the ligament*

The variations of normalized hydrostatic stress, $\sigma_h/\sigma_0 = \sigma_{kk}/3\sigma_0$, along the ligament connecting the notch tip and hole are shown in Figs 3(a) and (b) for the mode I case corresponding to $T/\sigma_0 = 0$ and -0.75, respectively. Results are presented in these figures pertaining to different load levels $J/(\sigma_0 L)$. In these and the following figures, the distance x is measured along the ligament from the centre of curvature of the notch in the undeformed configuration. The extent of the ligament goes from $x/L = 0.1$–0.9 and the curves displayed in these figures cover the range of x/L from 0.109–0.891. This affords resolution of the strain fields very close to the notch tip and the hole as will be seen subsequently.

It can be seen from Fig. 3(a) that for $T/\sigma_0 = 0$, a large peak hydrostatic stress (around $2.5\sigma_0$) is attained in the middle of the ligament even when the load $J/(\sigma_0 L) = 0.04$. The peak value saturates at around $3\sigma_0$ with further increase in load. The distribution of hydrostatic stress in the ligament for positive T-stress (like $T/\sigma_0 = +0.75$), is very similar to Fig. 3(a). On examining Fig. 3(b), it can be seen that, for the case of $T/\sigma_0 = -0.75$, the peak hydrostatic stress at $J/(\sigma_0 L) = 0.04$ occurs just ahead of the notch tip and is around $1.8\sigma_0$, whereas, the predominant portion of the ligament

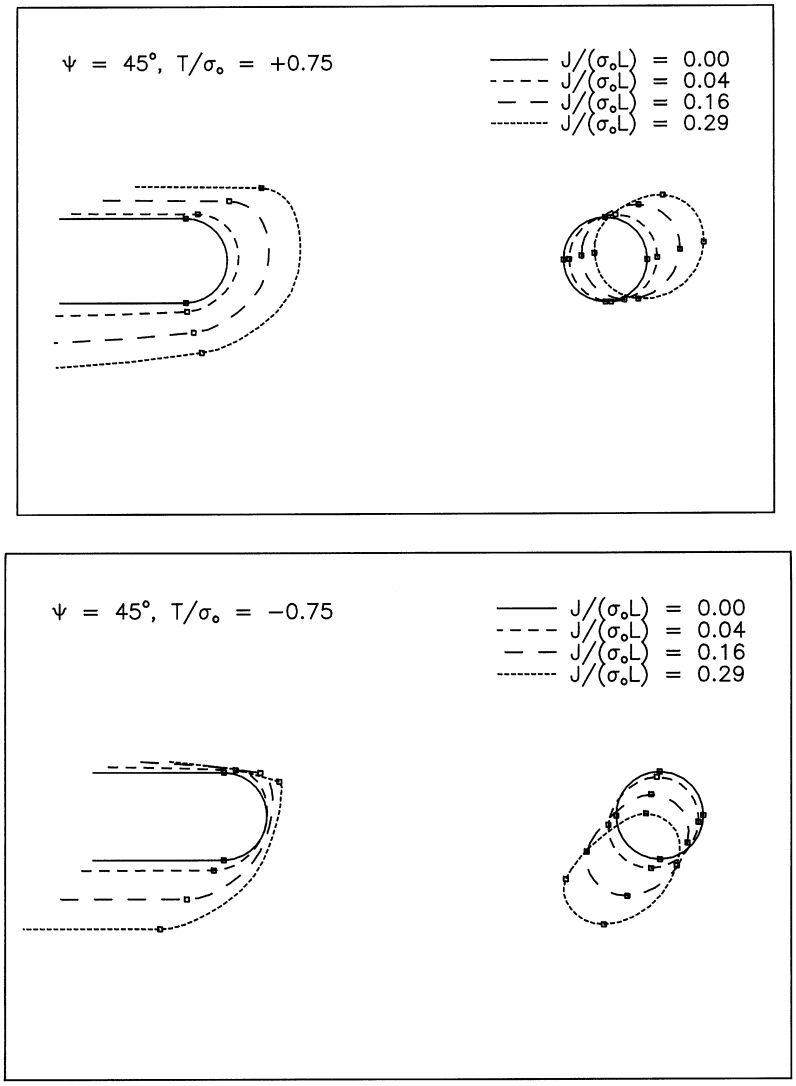

Fig. 2. Deformed shapes of the notch and the hole at different load levels for (a) $\Psi = 45^\circ$, $T/\sigma_0 = +0.75$ and (b) $\Psi = 45^\circ$, $T/\sigma_0 = -0.75$.

experiences much lower hydrostatic stress (less than $1.5\sigma_0$). The magnitude of σ_h in the central portion of the ligament elevates with increase in $J/(\sigma_0 L)$ and attains a peak value of around $2.5\sigma_0$ at $J/(\sigma_0 L) = 0.29$. Thus, there is a reduction of hydrostatic stress level in the ligament when the T-stress is negative, which corroborates with the negative Q-stress predicted by O'Dowd and Shih (1992).

The distribution of equivalent plastic strain $\bar{\varepsilon}_p = \int \sqrt{(\frac{2}{3} D^p_{ij} D^p_{ij})}\, \mathrm{d}t$ in the ligament for the mode I analysis at different load levels are displayed in Figs 4(a) and (b) for $T/\sigma_0 = 0$ and -0.75, respectively. Again, the results for positive T-stress are very close to $T/\sigma_0 = 0$ and are not presented

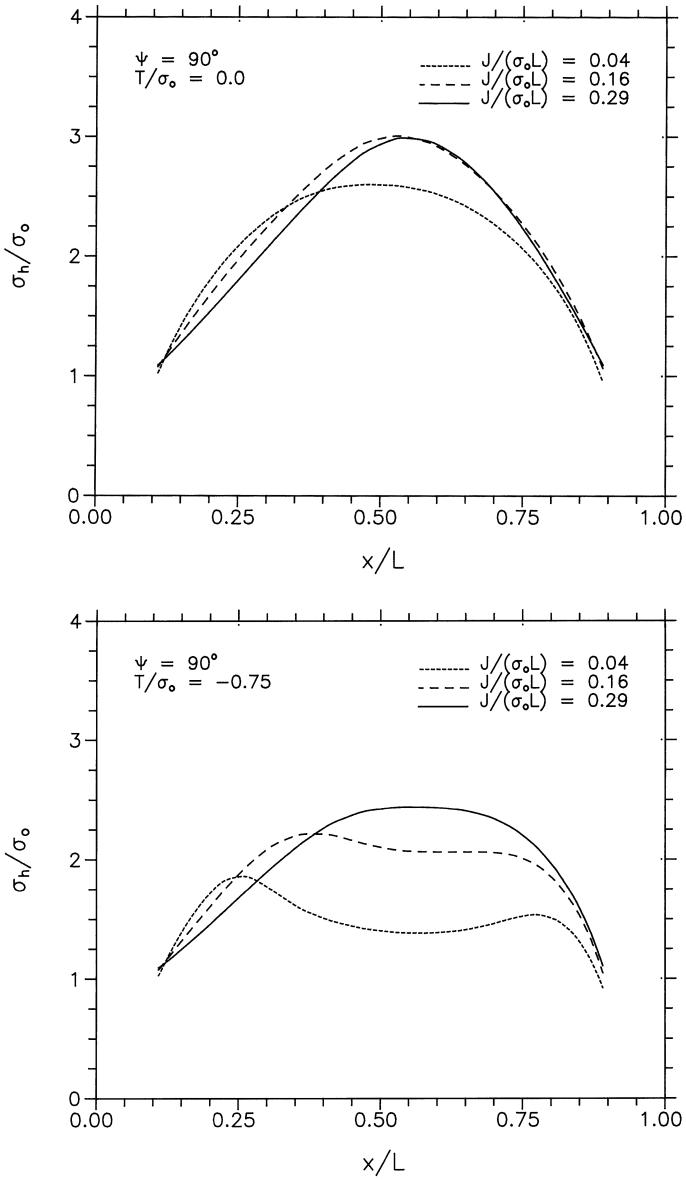

Fig. 3. Distribution of normalized hydrostatic stress (σ_h/σ_0) along the ligament connecting the notch tip and the hole at different load levels for (a) $\Psi = 90^\circ$, $T/\sigma_0 = 0$ and (b) $\Psi = 90^\circ$, $T/\sigma_0 = -0.75$.

here. It should be first observed from Figs 4(a) and (b) that, with increase in $J/(\sigma_0 L)$, the plastic strain near the notch tip as well as near the hole elevates dramatically. The magnitude of $\bar{\varepsilon}_p$ at the notch tip for the case of negative T-stress (Fig. 4(b)) is marginally higher than that for $T/\sigma_0 = 0$ (Fig. 4(a)) at a given $J/(\sigma_0 L)$. This is attributed to the larger blunting of the notch when the T-stress is negative as will be seen later. However, while the plastic strain in the central portion of

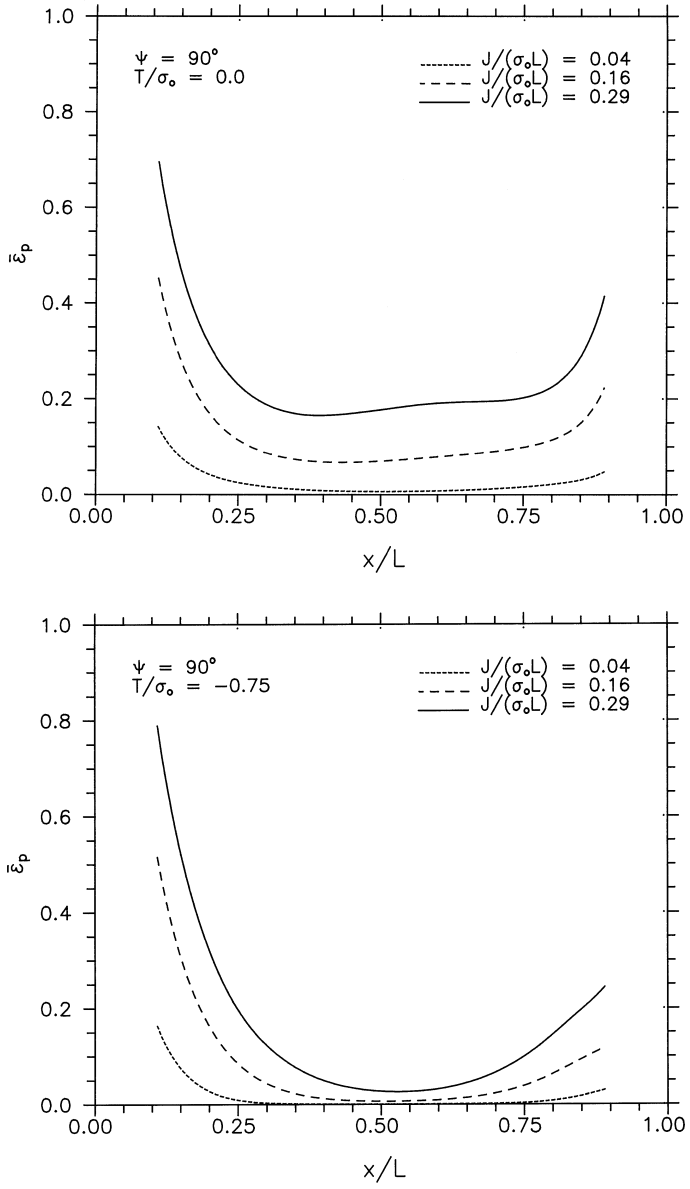

Fig. 4. Distribution of equivalent plastic strain $\bar{\varepsilon}_p$ along the ligament connecting the notch tip and the hole at different load levels for (a) $\Psi = 90^\circ$, $T/\sigma_0 = 0$ and (b) $\Psi = 90^\circ$, $T/\sigma_0 = -0.75$.

the ligament also elevates substantially for $T/\sigma_0 = 0$ (as well as for positive T-stress) with increase in load level, it is found from Fig. 4(b) that, $\bar{\varepsilon}_p$ increases very slowly in the predominant part of the ligament for the case of negative T-stress. In other words, plastic strain localization in the ligament due to the interaction between the notch and hole for mode I occurs more slowly when

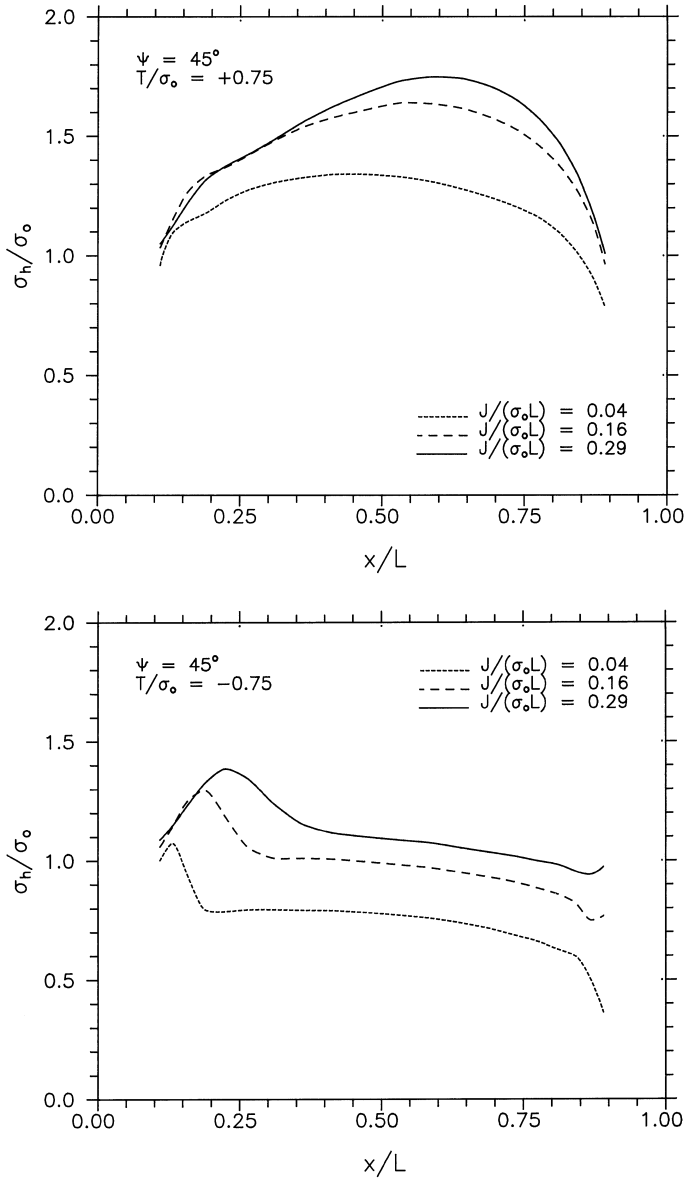

Fig. 5. Distribution of normalized hydrostatic stress (σ_h/σ_0) along the ligament connecting the notch tip and the hole at different load levels for (a) $\Psi = 45^\circ$, $T/\sigma_0 = +0.75$ and (b) $\Psi = 45^\circ$, $T/\sigma_0 = -0.75$.

the T-stress is negative. This has important implications on the growth of the hole (as will be seen later) and on the failure of the ligament due to micro-void coalescence.

The variations of normalized hydrostatic stress in the ligament for the mixed mode case $\Psi = 45^\circ$ are shown in Figs 5(a) and (b) corresponding to $T/\sigma_0 = +0.75$ and -0.75, respectively. It can be

noticed from Fig. 5(a) that for $T/\sigma_0 = +0.75$, the distribution of σ_h/σ_0 in the ligament is similar to the mode I case (see Figs 3), although the peak value attained is much less and is around $1.8\sigma_0$. This gives rise to a more or less rounded shape for the hole as discussed in connection with Fig. 2(a) for $\Psi = 45^\circ$ and $T/\sigma_0 = +0.75$, which resembles the results for the mode I case (see, for example, Ghosal and Narasimhan, 1996). On the other hand, it can be noticed from Fig. 5(b) that, the variation of σ_h/σ_0 in the ligament for $\Psi = 45^\circ$ decreases radially away from the notch tip when T/σ_0 is negative. Further, the maximum value of σ_h/σ_0 in the ligament is quite low for this case.

Interestingly, unlike mode I, the results corresponding to negative T-stress for the mixed mode case $\Psi = 45^\circ$ are closer to those for $T/\sigma_0 = 0$. As mentioned earlier, a recent investigation (Arun Roy and Narasimhan, 1997) has shown that, the near-tip plastic mode mixity changes as a function of T-stress for a given Ψ. Thus, the change in the peak hydrostatic stress in the ligament with T-stress for mixed mode loading is not because of loss of J-dominance as observed by O'Dowd and Shih (1991) for mode I, but is due to the above noted alteration in near-tip mode mixity.

In Figs 6(a–c), the distribution of plastic strain in the ligament at different load levels are shown for the case $\Psi = 45^\circ$ corresponding to $T/\sigma_0 = +0.75$, 0 and -0.75, respectively. On comparing Figs 6(a) and (b), it can be seen that, the accumulation of plastic strain in the ligament (with respect to $J/(\sigma_0 L)$) is much slower when the T-stress is positive. On the other hand, it can be noticed from Figs 6(b) and (c) that, an imposition of negative T-stress only marginally elevates the plastic strain distribution at a given $J/(\sigma_0 L)$. This implies that the localization of plastic strain in the ligament for the mixed mode case $\Psi = 45^\circ$ is retarded if a positive T-stress is imposed. This may be traced to the change in near-tip mode mixity towards mode I when the T-stress is positive (see Arun Roy and Narasimhan, 1997), which impedes development of intense shear deformation in the ligament.

On comparing Figs 4 and 6, it can be observed that the plastic strain develops faster in the ligament under mixed mode loading than mode I. This effect is not so pronounced when a positive T-stress is imposed, but it is quite significant when the T-stress is zero or negative. The above faster localization of plastic strains for mixed mode loading with a high mode II component is attributed to the intense shear deformation in the ligament.

The variations of normalized hydrostatic stress in the ligament at different load levels are shown in Fig. 7 for the mixed mode case $\Psi = 30^\circ$ corresponding to $T/\sigma_0 = 0$. It is clear from this figure that σ_h/σ_0 is very low for $\Psi = 30^\circ$ (with a peak value of around 1.2 at $J(\sigma_0 L) = 0.29$) as compared to mode I (Figs 3) and $\Psi = 45^\circ$ (Figs 5). Further, the hydrostatic stress variation in the ligament for $\Psi = 30^\circ$ changes only marginally when a positive or negative T-stress is imposed.

The distributions of equivalent plastic strain in the ligament for $\Psi = 30^\circ$ are presented in Fig. 8(a) and (b), corresponding to $T/\sigma_0 = +0.75$ and -0.75, respectively. It can be seen from these figures that, as in the case of $\Psi = 45^\circ$, the plastic strain variation in the ligament at a given $J/(\sigma_0 L)$ is higher when the T-stress is negative. However, unlike $\Psi = 45^\circ$, the above effect is much less pronounced for $\Psi = 30^\circ$. Thus, at the same $J/(\sigma_0 L)$ values, $\bar{\varepsilon}_p$ for $T/\sigma_0 = -0.75$ (Fig. 8(b)) is only around 20% higher than that for $T/\sigma_0 = +0.75$ (Fig. 8(a)). Hence, it may be concluded that under mixed mode loading with a very high mode II component, the hydrostatic stress is low and the development of plastic strain in the ligament is rapid, irrespective of the magnitude and sign of the T-stress.

On comparing Figs 4(a) and (b) with Figs (6a–c) and 8(a) and (b), it can be noticed that, with mode I predominant loading, there is a tendency for the plastic strain to increase sharply as the

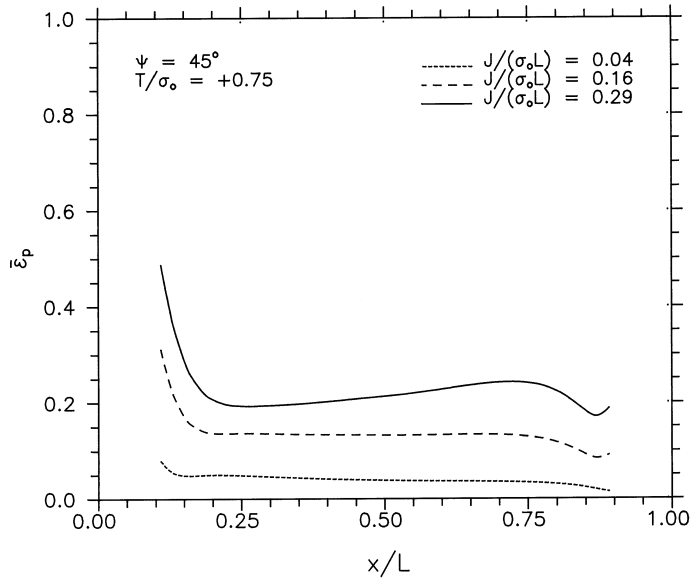

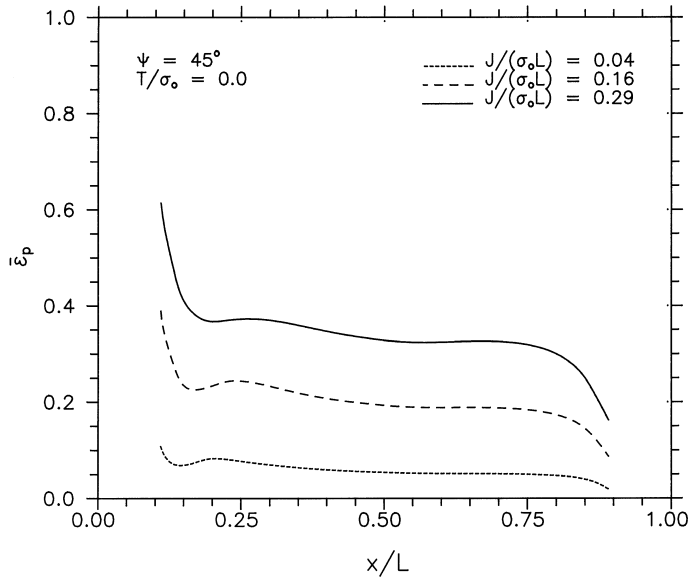

Fig. 6. Distribution of equivalent plastic strain $\bar{\varepsilon}_p$ along the ligament connecting the notch tip and the hole at different load levels for (a) $\Psi = 45^\circ$, $T/\sigma_0 = +0.75$ and (b) $\Psi = 45^\circ$, $T/\sigma_0 = 0$ and (c) $\Psi = 45^\circ$, $T/\sigma_0 = -0.75$.

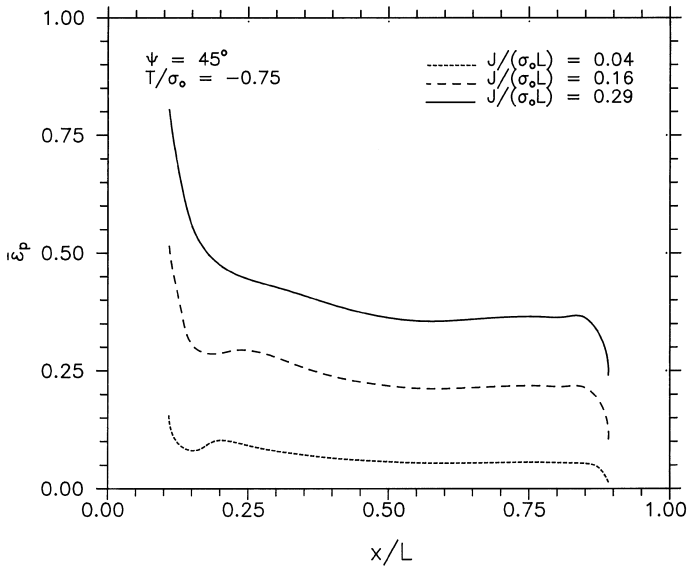

Fig. 6. Continued.

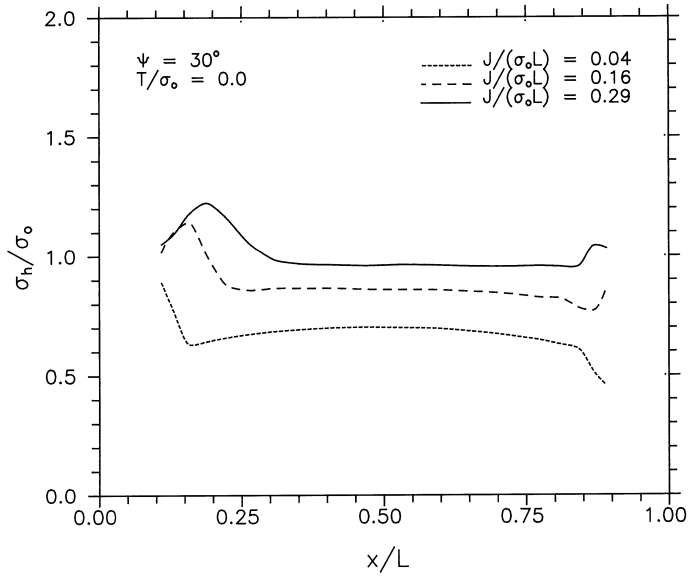

Fig. 7. Distribution of normalized hydrostatic stress (σ_h/σ_0) along the ligament connecting the notch tip and the hole at different load levels for $\Psi = 30^\circ$ and $T/\sigma_0 = 0$.

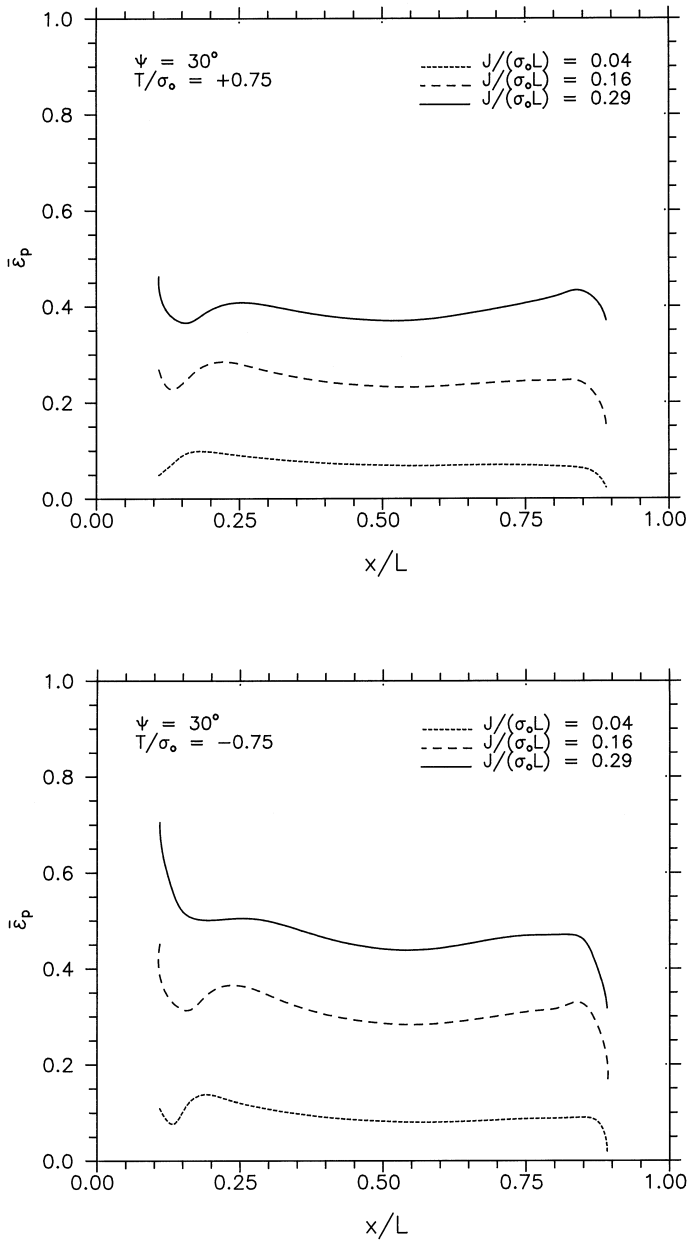

Fig. 8. Distribution of equivalent plastic strain $\bar{\varepsilon}_p$ along the ligament connecting the notch tip and the hole at different load levels for (a) $\Psi = 30^\circ$, $T/\sigma_0 = +0.75$ and (b) $\Psi = 30^\circ$, $T/\sigma_0 = -0.75$.

notch tip is approached. By contrast, for mode II predominant loading (see Figs 8(a) and (b)), the plastic strain appears to be uniformly high over the entire ligament.

4.3. *Notch opening and hole growth*

The notch diameter b, normalized by the initial value b_0, is plotted as a function of the load parameter $J/(\sigma_0 L)$ for the mode I case in Fig. 9a. Here, the notch diameter b represents the distance between two points which in the undeformed configuration are located above and below its centre of curvature (marked as P_0 and Q_0 in Fig. 1). The variations of the normalized maximum hole diameter, a_{max}/a_0 (where, a_0 is the initial diameter), with respect to $J/(\sigma_0 L)$ are shown in Fig. 9b. Results are presented in these figures corresponding to $T/\sigma_0 = +0.75$, 0, and -0.75. It can be seen from Fig. 9a that the normalized notch diameter at a given $J/(\sigma_0 L)$ is almost the same for positive and zero T-stress, while it is slightly higher for negative T-stress. This agrees with the marginally higher plastic strain just ahead of the notch tip when the T-stress is negative (see Figs 4(a) and (b)). The higher notch opening at a given $J/(\sigma_0 L)$ for the case of negative T-stress under mode I loading has also been reported by O'Dowd and Shih (1992), and O'Dowd (1995). O'Dowd (1995) has employed this result along with a fracture criterion based on the attainment of a critical crack tip opening displacement and has predicted that the value of J at fracture initiation (due to ductile failure) is lower if the T-stress (or Q-stress) is negative.

On the contrary, it can be seen from Fig. 9b that the normalized maximum diameter of the hole, a_{max}/a_0, corresponding to $T/\sigma_0 = -0.75$ grows much more slowly with respect to $J/(\sigma_0 L)$ as compared to $T/\sigma_0 = 0$. The hole growth rate for the case $T/\sigma_0 = +0.75$ is marginally higher than $T/\sigma_0 = 0$. The above observation can be rationalized by recalling that there is lower hydrostatic stress and slower plastic strain development in the ligament for the mode I case if the T-stress is negative.

The trends noted above are expected to reflect on porosity accumulation and consequent failure of the ligament by micro-void coalescence. Thus, the value of J at fracture initiation due to micro-void coalescence under mode I loading is expected to increase if the T-stress is negative. On the other hand, positive T-stress can slightly decrease the mode I fracture toughness due to failure by ductile void coalescence. It must be mentioned here that while the predictions of O'Dowd (1995) are based purely on the notch opening displacement, the present analysis is more realistic since the interaction between a notch and hole has been modelled.

The evolution of the normalized maximum hole diameter, a_{max}/a_0, is shown in Figs 10(a) and (b) as a function of the load parameter $J/(\sigma_0 L)$ for two mixed mode cases, $\Psi = 45$ and 30°, respectively. Results are presented in these figures corresponding to different T/σ_0 values. The rate of hole growth for positive T-stress is less than that pertaining to negative and zero T-stress values. The above effect is more pronounced for $\Psi = 45^\circ$ as compared to $\Psi = 30^\circ$. This trend is in contrast to the results for mode I loading (Fig. 9b) where positive T-stress increases the hole growth rate above that for zero and negative T-stress.

The slower evolution of the hole diameter with respect to $J/(\sigma_0 L)$ when positive T-stress is imposed under mixed mode loading (at a fixed $\Psi < 90^\circ$) is traced to a shift in the near-tip plastic mixity closer to that for mode I (see Arun Roy and Narasimhan, 1997). As already mentioned, this retards the localization of plastic flow due to shear deformation in the ligament. Further, as

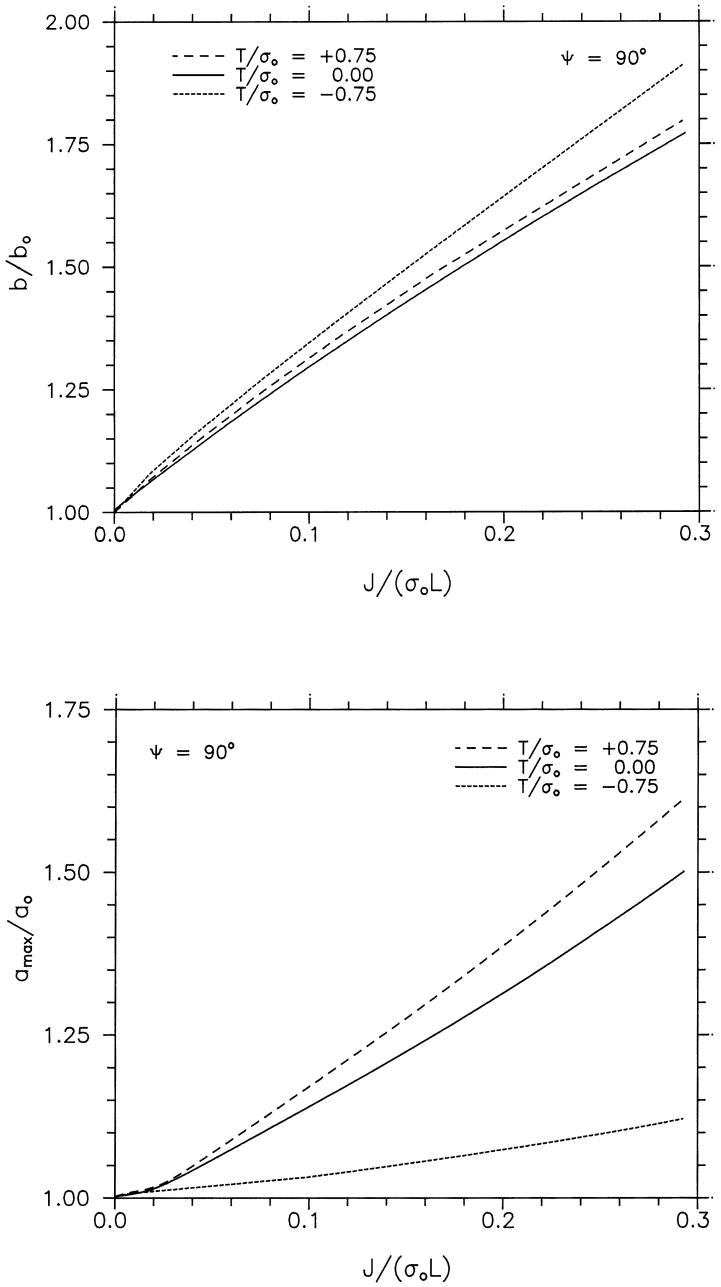

Fig. 9. (a) Variation of normalized notch diameter b/b_0, with the normalized loading parameter $J/(\sigma_0 L)$ corresponding to $\Psi = 90^\circ$ (mode I) for different T/σ_0. (b) Evolution of normalized maximum hole diameter, $a_{\max}/a_0$, with $J/(\sigma_0 L)$ corresponding to $\Psi = 90^\circ$ for different T/σ_0.

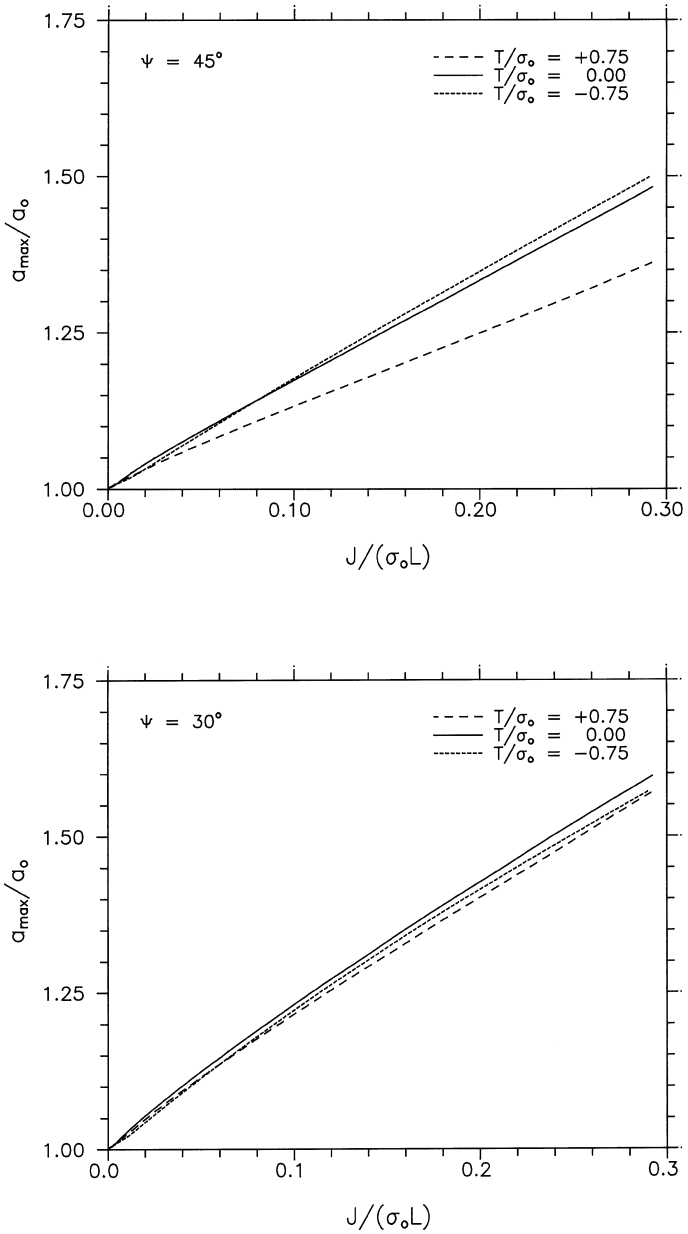

Fig. 10. Evolution of normalized maximum hole diameter, a_{max}/a_0 with $J/(\sigma_0 L)$ for different T/σ_0 corresponding to (a) $\Psi = 45^\circ$ and (b) $\Psi = 30^\circ$.

discussed in connection with Figs 6 and 8, this effect is more pronounced for $\Psi = 45^\circ$ as compared to $\Psi = 30^\circ$. For the case of $\Psi = 30^\circ$ (which has a high mode II component of loading), it can be observed from Fig. 10b that, the T-stress has negligible effect on the evolution of the maximum hole diameter with respect to $J/(\sigma_0 L)$.

On comparing Figs 9b, 10(a) and 10(b), for negative and zero T-stress values the hole growth rate is elevated as the mode II component of loading is increased. The above trend is significant for the case of negative T-stress. In contrast, for the positive T-stress it is found that as Ψ decreases initially from 90°, there is a retardation of the rate of hole growth. With further decrease in Ψ, the evolution rate of the hole increases and, in fact, becomes higher than that for mode I.

The above results imply that under mixed mode loading (at a given $\Psi < 90^\circ$), ductile fracture initiation will be impeded if the T-stress is positive. However, under predominantly mode II loading, the T-stress will have negligible effect on the ductile fracture process. Further, for negative and zero T-stress, an increase in mode II component of loading is expected to reduce the value of J at fracture initiation due to micro-void coalescence. On the other hand, for positive T-stress, the ductile fracture toughness is expected to increase as Ψ decreased initially from 90°. With further decrease in Ψ, it is expected to decrease considerably.

4.4. *Growth of hole oriented at an angle*

It is important to understand whether a hole present at an angle with respect to the notch line (in particular, on the blunted side of the notch) grows faster as compared to a hole located directly ahead of the notch tip. To this end, finite element analyses of the interaction between the notch and a hole located at an angle of $\theta = -30^\circ$ with respect to the notch line (i.e., near the blunted part) under mixed mode loading have been conducted. The initial hole diameter, a_0, and the spacing between the centre of curvature of the notch and the hole, L, are kept the same as in the previous analysis.

The evolution histories of the normalized maximum diameter, $a_{\max}/a_0$, of a hole located directly ahead of the notch tip are compared against those for a hole inclined at an angle of $\theta = -30^\circ$ in Fig. 11. Results are presented in this figure for different values of mode mixities Ψ pertaining to the case $T/\sigma_0 = 0$. It can be clearly seen from this figure that a hole located directly ahead of the notch tip grows faster (with respect to $J/(\sigma_0 L)$) compared to a hole at an angle irrespective of the mode mixity parameter, Ψ. Results of hole growth for other values of T/σ_0 (like -0.75 and $+0.75$) are found to exhibit similar trends.

A typical plot which illustrates the distribution of equivalent plastic strain in the region between the notch tip and the hole, inclined at $\theta = -30^\circ$ is shown in Fig. 12. This figure pertains to the mixed mode case $\Psi = 30^\circ$ and $T/\sigma_0 = 0$. On comparing this figure with Figs 8(a) and (b), it can be seen that, except in the region very near the notch tip, the plastic strain in the entire ligament for the hole at $\theta = 0^\circ$ is much higher in magnitude for the same value of $J/(\sigma_0 L)$. Thus, the plastic strain localization in the ligament for the hole at $\theta = 0^\circ$ occurs faster than that for the hole located at $\theta = -30^\circ$. This explains the reasons for the faster growth of the hole, when it is present directly ahead of the notch tip instead of at an angle on the blunted side of the notch.

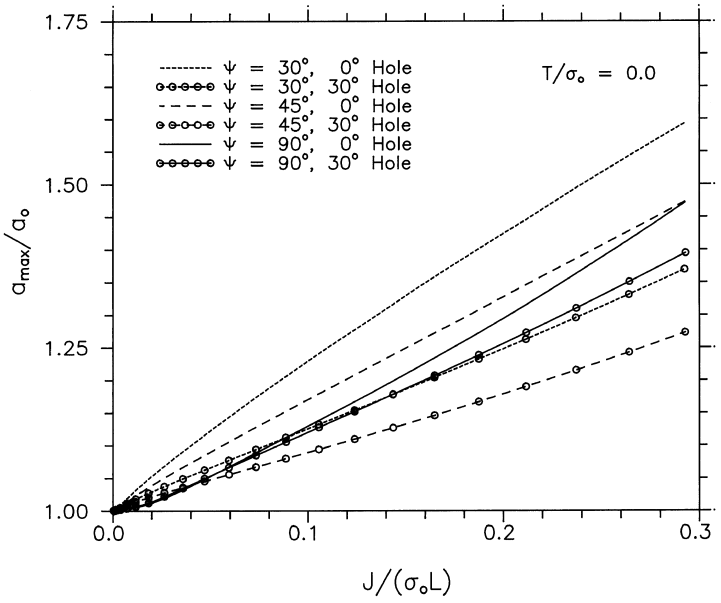

Fig. 11. Comparison of evolution histories of hole diameters for a hole located directly ahead of the notch tip (at $\theta = 0^\circ$) and a hole at an angle (at $\theta = -30^\circ$) corresponding to $T/\sigma_0 = 0$ and different values of Ψ.

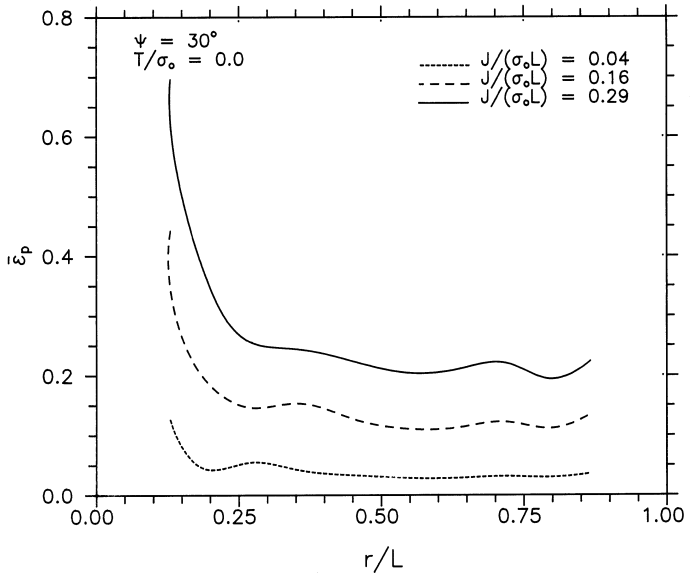

Fig. 12. Variation of equivalent plastic strain in the region between the notch tip and a hole located at $\theta = -30^\circ$ corresponding to different load levels for $\Psi = 30^\circ$ and $T/\sigma_0 = 0$.

5. Conclusions

In this work, large deformation finite element analyses have been carried out to study the effect of T-stress on the growth of a cylindrical hole near a notch tip under mixed mode loading conditions. The following are the main conclusions of these analyses.

Under mode I loading, the development of hydrostatic stress and the equivalent plastic strain in the ligament with respect to $J/(\sigma_0 L)$, for zero and positive T-stress greatly exceeds the levels for a negative T-stress. Consequently, the rate of hole growth with respect to $J/(\sigma_0 L)$ for negative T-stress is very much retarded.

Under mixed mode loading, plastic strain localization between the notch tip and the hole is accompanied by intense shear deformation. Unlike the mode I case, positive T-stress retards plastic flow localization in the ligament, whereas, for zero and negative T-stress, the plastic strain accumulation in the ligament is very rapid. Consequently, the rate of hole growth for zero and negative T-stress is higher than for positive T-stress. However, under predominantly mode II loading, T-stress has negligible effect on hole growth near the notch tip.

For negative and zero T-stress values, the hole growth rate is elevated as the mode II component of loading is increased. On the contrary, for positive T-stress, it is found that as Ψ decreases initially from 90°, there is a retardation of hole growth. With further decrease in Ψ, the hole growth increases and becomes higher than that for mode I.

Acknowledgement

The authors would like to gratefully acknowledge the Aeronautics Research and Development Board (Government of India) for financial support through sponsored project no. Aero/RD-134/100/10/96-97/778.

References

Aravas, N., McMeeking, R.M., 1985a. Finite element analysis of void growth near a blunting crack-tip. J. Mech. Phys. Solids 33, 25–49.

Aravas, N., McMeeking, R.M., 1985b. Microvoid growth and failure in the ligament between hole and a blunt crack-tip. Int. J. Fracture 24, 25–38.

Arun Roy, Y., Narasimhan, R., 1997. J-dominance in mixed mode ductile fracture specimens. Int. J. Fracture, accepted for publication.

Betegon, C., Hancock, J.W., 1991. Two-parameter characterization of elastic–plastic crack tip fields. J. Appl. Mech. 58, 104–110.

Garrison, W.M., Jr., Moody, N.R., 1987. Ductile fracture. J. Phys. Chem. Solids 48, 1035–1074.

Ghosal, A.K., Narasimhan, R., 1996. Numerical simulations of hole growth and ductile fracture initiation under mixed mode loading. Int. J. Fracture 77, 281–304.

Ghosal, A.K., Narasimhan, R., 1997. A finite element study of the effect of void initiation and growth on mixed mode ductile fracture. Mech. Mater. 25, 113–127.

Gurson, A.L., 1977. Continuum theory of ductile rupture by void nucleation and growth—Part I. Yield criterion and flow rules for porous ductile media. J. Engng Mater. Technol. 99, 2–15.

Hughes, T.J.R., 1980. Generalization of selective integration procedures to anisotropic and nonlinear media. Int. J. Num. Meth. Engng 15, 1413–1418.

Hughes, T.J.R., Winget, J., 1980. Finite rotation effects in numerical integration of rate constitutive equations arising in large deformation analysis. Int. J. Num. Meth. Engng 15, 1862–1867.

McMeeking, R.M., Rice, J.R., 1975. Finite element formulations for problems of large elastic–plastic deformations. Int. J. Solids Structures 11, 601–616.

O'Dowd, N.P., 1995. Applications of two parameter approaches in elastic–plastic fracture mechanics. Engng Fracture Mech. 52, 445–465.

O'Dowd, N.P., Shih, C.F., 1991. Family of crack tip fields characterized by a triaxiality parameter—I. Structure of fields. J. Mech. Phys. Solids 39, 989–1015.

O'Dowd, N.P., Shih, C.F., 1992. Family of crack tip fields characterized by a triaxiality parameter—II. Fracture applications. J. Mech. Phys. Solids 40, 939–963.

Rice, J.R., Johnson, M.A., 1970. The role of large crack-tip geometry changes in plane strain fracture. In: Kanninen, M.F., Adler, W.F., Rosenfield, A.R., Jaffe, R.I. (Eds.), Inelastic Behaviour of Solids. New York: McGraw-Hill Series in Material Science and Engineering, pp. 641–672.

Shih, C.F., 1974. Small scale yielding analysis of mixed mode plane strain crack problems. ASTM STP 560, 187–210.

Tvergaard, V., Hutchinson, J.W., 1994. Effect of *T*-stress on mode I crack growth resistance in a ductile solid. Int. J. Solids and Structures 31, 823–833.

Van Stone, R.H., Cox, T.B., Low, J.R., Jr., Psioda, J.A., 1985. Microstructural aspects of fracture by dimpled rupture. Int. Met. Reviews 30, 157–179.

Williams, M.L., 1957. On the stress distribution at the base of a stationary crack. J. App. Mech. 24, 111–114.

Xia, L., Shih, C.F., 1995a. Ductile crack growth—I. A numerical study using computational cells with microstructurally-based length scales. J. Mech. Phys. Solids 43, 233–259.

Xia, L., Shih, C.F., 1995b. Ductile crack growth—II. Void nucleation and geometry effects on macroscopic fracture behavior. J. Mech. Phys. Solids 43, 1953–1981.